# Instability of Hall MHD Generators to Magneto-Acoustic Waves

FRANK J. FISHMAN*
*Avco Everett Research Laboratory, Everett, Mass.*

**It is known that magneto-acoustic waves propagating antiparallel to a steady electric current in a dense, weakly ionized gas may exhibit substantial growth. In this paper, the stability of a Hall MHD generator with supersonic flow to disturbances of this type is assessed. A proper boundary-value problem for an unsteady, one-dimensional model of such a generator is solved, with full consideration of the load circuit, which may serve as a feedback path for wave energy. It is shown that this feedback may lead to instabilities even under conditions such that the wave growth (as evaluated by earlier investigations) is slow. Disturbances with a period comparable to the flow time (channel length/fluid velocity) are the principal contributors to the instability; the spatial variation of these disturbances are far from sinusoidal. The control of machine instabilities by electrical filters in the external (load) circuit is described.**

## Introduction

MAGNETO-acoustic waves, propagating pressure fluctuations which in the limit of small MHD interaction become normal acoustic waves, may exhibit growth in dense, weakly ionized plasmas with strong electric currents and magnetic fields. Perturbation currents interacting with the magnetic field, when properly phased with the pressure fluctuations, lead to growth. Velikhov first called attention to the possible importance of such waves for MHD electric power generators and discussed a growth mechanism involving perturbation currents due to fluctuations of the Hall parameter with density fluctuations.[1] McCune generalized the concept to include fluctuations of all plasmas properties which depend on the thermodynamic properties of the gas, and noted that in many circumstances conductivity fluctuations may provide the dominant mechanism of wave growth.[2] Recognizing that conditions in Hall MHD generators were especially favorable to growth of axial waves of this type, Locke and McCune examined wave growth under plasma conditions appropriate to such machines and attempted to estimate the effects of the axial plasma inhomogeneities that exist in useful generators.[3] More recently, Powers and Dicks have published somewhat more refined calculations of axial wave growth in the segmented diagonal connected generator (which includes the Hall generator as a special case) and have emphasized the possible growth of the entropy wave.[4]

The works cited here are inadequate to assess Hall generator stability on two grounds. The more basic of the two is that these authors only treated wave growth in an essentially infinite medium. Although it seems clear that a mechanism of wave growth is a necessary condition of over-all machine instability, there is no easy way to estimate what growth rate will lead to instability. This quantitative question certainly depends on the nature of the generator load circuit, which may serve as a feedback path for wave energy, allowing continued growth even for slowly growing waves. An assessment of the stability of a finite machine calls for the solution of a proper boundary-value problem, including a correct treatment of the load circuit, rather than the simple determination of the unbounded plasma eigenfunctions. McCune has treated the effects of boundaries and load connection for transverse waves in a Faraday generator.[5] The linearized boundary-value problem for axial, magneto-acoustic disturbances in Hall generators with supersonic flow is the subject of this paper. It should be noted that in this paper "boundary" refers to the entrance or exit condition; the side wall "boundaries" are treated (or neglected) in the same way as in other channel flow calculations.

The other shortcoming of previous studies has been their limitation to short wavelength (high-frequency) disturbances. The present work, which is valid for arbitrarily low frequencies, indicates that disturbances with period comparable to the flow time (channel length/fluid velocity) generally are the most liable to lead to instability. In a Hall generator with significant MHD interaction, the spatial variation of these waves does not permit WKB-type treatments.[4] The axial variations of plasma velocity and thermodynamic properties inherent in the steady generator flow must be treated correctly, for they may dominate the growth of the important low-frequency waves.

The procedure adopted in the present work is as follows. The general equations describing time-dependent channel flow are written down. The steady solution of these equations, corresponding to the usual Hall generator channel flow, is determined. The equations describing small time-dependent departures from this solution are derived. Because of the prescribed linear nature of these equations, a complex exponential time dependence of the solution may be assumed; a similar spatial dependence is not permitted because the coefficients appearing in the equations have a spatial dependence prescribed by the steady solution. The resulting ordinary linear differential equations are solved subject to the appropriate boundary conditions to determine the spatial dependence of the perturbation. The axial electric field thus determined is integrated over the channel length to find the perturbation Hall voltage. The ratio of this voltage to the perturbation axial current is the external load impedance at the assumed frequency that will lead to the assumed time dependence. Thus, the time dependence of a disturbance in a channel with fixed external connections is indirectly calculated. This indirect calculation is relatively convenient since the primary object is to determine stability: stability is assured if the load circuit that corresponds to a purely periodic disturbance requires active elements (energy sources).

Received February 3, 1969; revision received June 20, 1969. The author wishes to acknowledge numerous clarifying conversations with E. V. Locke and J. E. McCune over the past 4 years. He is especially indebted to R. D. Gillespie, who efficiently and sympathetically bridged the communications gap with the IMB System 360 installed at Avco Everett Research Laboratory.

* Principal Research Scientist; presently Associate Professor, Physics Department, Adrian College, Adrian, Mich.

## Method of Analysis

The equations of unsteady magnetohydrodynamic channel flow are

$$A(\partial\rho/\partial t) + (\partial/\partial x)(\rho u A) = 0 \quad (1)$$

$$\rho[(\partial/\partial t) + u(\partial/\partial x)]u + (\partial p/\partial x) + j_z B = 0 \quad (2)$$

$$\rho[(\partial/\partial t) + u(\partial/\partial x)](h + u^2/2) - (\partial p/\partial t) = j_x E_x + j_z E_z \quad (3)$$

where viscosity and heat conductivity have been neglected. It is assumed that the channel cross-sectional area $A$ may be a slowly varying function of the axial coordinate $x$ but is time independent. The magnetic field $B$ is constant and normal to $x$ and $z$. The flow variables, axial velocity $u$, density $\rho$, pressure $p$, enthalpy $h$, along with the current density $\mathbf{j}$, and electric field $\mathbf{E}$ may be arbitrary functions of both $x$ and $t$. These quasi-one-dimensional equations are valid for all axial disturbances in channels of length $L$ much greater than a typical diameter ($\sim A^{1/2}$). Further, all disturbances of frequencies sufficiently low that their characteristic dimension is large compared to this diameter must be essentially axial and hence correctly described by these equations. The relevant Ohm's law is

$$j_x = \sigma(\rho,h)E_x + \omega\tau(\rho,h)j_z \quad (4)$$

$$j_z = \sigma(\rho,h)(E_z + uB) - \omega\tau(\rho,h)j_x \quad (5)$$

where the conductivity $\sigma$ and Hall parameter $\omega\tau$ are taken as general functions of the state parameters $\rho$ and $h$. Maxwell's equations require that the current density field be solenoidal and the electric field irrotational. For a Hall generator, the solenoidal nature of the current is simply expressed by the uniformity of the total axial current $J(t)$

$$J(t) = A(x)j_x(x,t) \quad (6)$$

where $j_x(x,t)$ is the axial current density averaged over the channel section. It is here assumed that the electric field $\mathbf{E}$ is a function of $x$ and $t$ alone; this is compatible with the field's necessary irrotational nature if either 1) the transverse field $E_z$ is small (we assume $E_y \equiv 0$) or 2) this field varies only slowly with $x$. In an ideal Hall generator, the transverse field vanishes identically, but in order to apply analyses of the present type to certain small experimental generators, it is necessary to allow for the effect of electrode voltage drop, which leads to transverse fields in the core of the gas.

The model of electrode drop adopted here is that there is a fixed voltage drop $V_e$ that always opposes current flow from the electrodes, and that when the net electromotive force across the channel is less than $V_e$, no current flows. This model, along with Ohm's law yields the following prescription for the transverse field:

$$\begin{aligned} V_i > V_e &\rightarrow E_z = -V_e/d \\ |V_i| < V_e &\rightarrow E_z = -uB + \omega\tau J/\sigma A \\ V_i < -V_e &\rightarrow E_z = V_e/d \end{aligned} \quad (7)$$

where $d(x)$ is the height of the channel in the $\mathbf{u} \times \mathbf{B}$ direction and

$$V_i = (uB - \omega\tau J/\sigma A)d \quad (8)$$

Thus, condition 1 previous is satisfied if $V_e \ll uBd$, whereas condition 2 is satisfied at low frequencies in any event.

Equations (4–7), can be used to eliminate the fields and current densities from Eqs. (1–3). If the pressure is eliminated from these by an equation of state of the form $p = p(\rho,h)$ there remains a system of three first-order equations involving the dependent variables $u, \rho, h, A, J$. These equations describe both the steady flow and the perturbation or stability analysis. These descriptions may be formally separated by assuming all variables have the form of a sum of a time independent part and a small part that is periodic in time, viz.,

$$\begin{aligned} J(t) &= J_0(1 + \epsilon e^{i\omega t}) \\ u(x,t) &= u_1(x) + \epsilon u_2(x)e^{i\omega t} \\ \rho(x,t) &= \rho_1(x) + \epsilon\rho_2(x)e^{i\omega t} \\ h(x,t) &= h_1(x) + \epsilon h_2(x)e^{i\omega t} \end{aligned} \quad (9)$$

where the linearization parameter $\epsilon$ is an arbitrary but small number. It should be emphasized that the $x$ dependence of both the steady flow and the perturbation remain general; there is no assumption of a propagation constant or "dispersion relation." It is convenient to define the quantities $A_0 = A(0)$, $u_0 = u_1(0)$, $\rho_0 = \rho_1(0)$, $h_0 = h_1(0)$, $\sigma_0 = \sigma(\rho_0,h_0)$, $\omega\tau_0 = \omega\tau(\rho_0,h_0)$ and use these to normalize the quantities appearing in the equations, namely $a = A/A_0$, $v_1 = u_1/u_0$, $v_2 = u_2/u_0$, $r_1 = \rho_1/\rho_0$, $r_2 = \rho_2/\rho_0$, $\theta_1 = h_1/h_0$, $\theta_2 = h_2/h_0$, $\xi = x/L$, and $w = \omega L/u_0$. The interaction parameter $S = \sigma_0 LB^2/\rho_0 u_0$ and the inlet loading parameter $\alpha_0 = \omega\tau_0 J_0/\sigma_0 A_0 u_0 B$ emerge as fundamental parameters from this normalization. Requiring that the dynamic equations hold separately for terms of order $\epsilon^0$ and $\epsilon^1$ leads to the separation into steady and stability analyses, respectively. The steady-flow equations are

$$(d/d\xi)(r_1 v_1 a) = 0 \quad (10)$$

$$r_1 v_1 \frac{dv_1}{d\xi} + \frac{1}{u_0^2}\frac{\partial p}{\partial \rho}\frac{dr_1}{d\xi} + \frac{h_0}{\rho_0 u_0^2}\frac{\partial p}{\partial h}\frac{d\theta_1}{d\xi} = S\psi_1 \quad (11)$$

$$(h_0/u_0^2)(d\theta_1/d\xi) + v_1(dv_1/d\xi) = S\Gamma_1 \quad (12)$$

where

$$V_i > V_e \rightarrow \psi_1 = -\frac{\sigma_1}{\sigma_0}v_1 + \frac{\sigma_1}{\sigma_0}\frac{V_e}{u_0 Bd} + \alpha_0\frac{\omega\tau_1}{\omega\tau_0}r_1 v_1$$

$$\Gamma_1 = \alpha_0\left[\alpha_0\frac{\sigma_0}{\sigma_1}\frac{1+\omega\tau_1^2}{\omega\tau_0^2}r_1 v_1 - \frac{\omega\tau_1}{\omega\tau_0}\left(v_1 - \frac{2V_e}{u_0 Bd}\right) - \frac{1}{r_1 v_1}\frac{\sigma_1}{\sigma_0}\frac{V_e}{u_0 Bd}\left(v_1 - \frac{V_e}{u_0 Bd}\right)\right]$$

$$|V_i| < V_e \rightarrow \psi_1 = 0,\ \Gamma_1 = (\alpha_0^2/\omega\tau_0^2)r_1 v_1$$

The perturbation equations are

$$r_1\frac{dv_2}{d\xi} + v_1\frac{dr_2}{d\xi} = \frac{r_1}{v_1}\frac{dv_1}{d\xi}v_2 - \left(iw - \frac{v_1}{r_1}\frac{dr_1}{d\xi}\right)r_2 \quad (13)$$

$$r_1 v_1\frac{dv_2}{d\xi} + \frac{1}{u_0^2}\frac{\partial p}{\partial\rho}\frac{dr_2}{d\xi} + \frac{h_0}{\rho_0 u_0^2}\frac{\partial p}{\partial h}\frac{d\theta_2}{d\xi} = -\left(iwr_1 + r_1\frac{dv_1}{d\xi}\right)v_2 - \left(v_1\frac{dv_1}{d\xi} + \frac{\rho_0}{u_0^2}\frac{\partial^2 p}{\partial\rho^2}\frac{dr_1}{d\xi} + \frac{h_0}{u_0^2}\frac{\partial^2 p}{\partial\rho\partial h}\frac{d\theta_1}{d\xi}\right)r_2 - \left(\frac{h_0}{u_0^2}\frac{\partial^2 p}{\partial\rho\partial h}\frac{dr_1}{d\xi} + \frac{h_0^2}{\rho_0 u_0^2}\frac{\partial^2 p}{\partial h^2}\frac{d\theta_1}{d\xi}\right)\theta_2 + S\psi_2 \quad (14)$$

$$v_1\frac{dv_2}{d\xi} + \frac{h_0}{u_0^2}\frac{d\theta_2}{d\xi} = -\left(iw + \frac{1}{v_1}\frac{h_0}{u_0^2}\frac{d\theta_1}{d\xi} + 2\frac{dv_1}{d\xi}\right)v_2 - \left(\frac{1}{r_1}\frac{h_0}{u_0^2}\frac{d\theta_1}{d\xi} + \frac{v_1}{r_1}\frac{dv_1}{d\xi} - \frac{iw}{r_1 v_1 u_0^2}\frac{\partial p}{\partial\rho}\right)r_2 - \frac{iw}{v_1}\frac{h_0}{u_0^2}\left(1 - \frac{1}{r_1\rho_0}\frac{\partial p}{\partial h}\right)\theta_2 + S\Gamma_2 \quad (15)$$

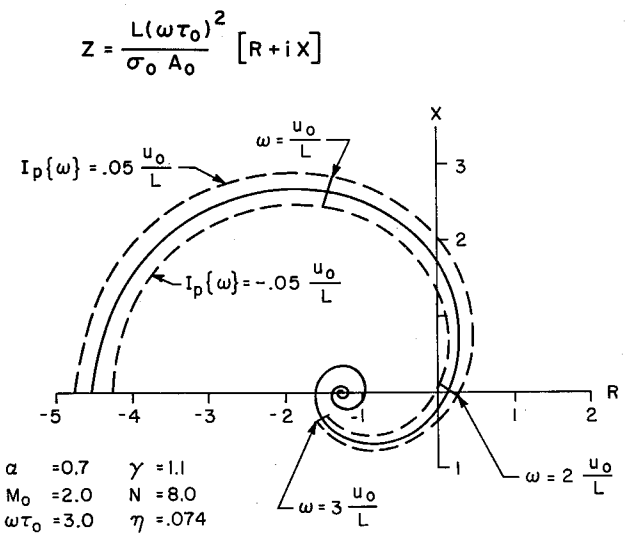


**Fig. 1 Complex perturbation impedance for idealized Hall generator. (The solid curve is the impedance locus for a periodic disturbance with disturbance angular frequency as the parameter. The dashed curves are for disturbances that have growth and decay times about 20 times the gas flow time. Impedance in the right half plane can be synthesized with passive elements.)**

where

$$V_i > V_e \rightarrow \psi_2 = -\frac{\sigma_1}{\sigma_0}v_2 - \left(\frac{\rho_0}{\sigma_0}\frac{\partial\sigma}{\partial\rho}v_1 - \frac{\rho_0}{\sigma_0}\frac{\partial\sigma}{\partial\rho}\times\frac{V_e}{u_0Bd} - \alpha_0\frac{\rho_0}{\omega\tau_0}\frac{\partial\omega\tau}{\partial\rho}r_1v_1\right)r_2 - \left(\frac{h_0}{\sigma_0}\frac{\partial\sigma}{\partial h}v_1 - \frac{h_0}{\sigma_0}\frac{\partial\sigma}{\partial h}\frac{V_e}{u_0Bd} - \alpha_0\frac{h_0}{\omega\tau_0}\frac{\partial\omega\tau}{\partial h}r_1v_1\right)\theta_2 + \alpha_0\frac{\omega\tau_1}{\omega\tau_0}r_1v_1$$

$$\Gamma_2 = -\left(\alpha_0\frac{\omega\tau_1}{\omega\tau_0} + \frac{V_e}{u_0Bd}\frac{\sigma_1}{\sigma_0}\frac{1}{r_1v_1}\right)v_2 - \alpha_0\left[-2\alpha_0\frac{\omega\tau_1}{\omega\tau_0^2}\times\frac{\sigma_0}{\sigma_1}\rho_0\frac{\partial\omega\tau}{\partial\rho}r_1v_1 + \alpha_0\left(\frac{\sigma_0}{\sigma_1}\right)^2\frac{1+\omega\tau_1^2}{\omega\tau_0^2}\frac{\rho_0}{\sigma_0}\frac{\partial\sigma}{\partial\rho}r_1v_1 + \frac{\rho_0}{\omega\tau_0}\frac{\partial\omega\tau}{\partial\rho}\left(v_1 - \frac{2V_e}{u_0Bd}\right) + \frac{1}{\alpha_0r_1v_1}\frac{V_e}{u_0Bd}\frac{\rho_0}{\sigma_0}\frac{\partial\sigma}{\partial\rho}\times\left(v_1 - \frac{V_e}{u_0Bd}\right)\right]r_2 - \alpha_0\left[-2\alpha_0\frac{\omega\tau_1}{\omega\tau_0^2}\frac{\sigma_0}{\sigma_1}h_0\frac{\partial\omega\tau}{\partial h}r_1v_1 + \alpha_0\left(\frac{\sigma_0}{\sigma_1}\right)^2\frac{1+\omega\tau_1^2}{\omega\tau_0^2}\frac{h_0}{\sigma_0}\frac{\partial\sigma}{\partial h}r_1v_1 + \frac{h_0}{\omega\tau_0}\frac{\partial\omega\tau}{\partial h}\left(v_1 - \frac{2V_e}{u_0Bd}\right) + \frac{1}{\alpha_0r_1v_1}\frac{V_e}{u_0Bd}\frac{h_0}{\sigma_0}\frac{\partial\sigma}{\partial h}\left(v_1 - \frac{V_e}{u_0Bd}\right)\right]\theta_2 + \alpha_0\left[2\alpha_0\frac{\sigma_0}{\sigma_1}\times\frac{1+\omega\tau_1^2}{\omega\tau_0^2}r_1v_1 - \frac{\omega\tau_1}{\omega\tau_0}\left(v_1 - \frac{2V_e}{u_0Bd}\right)\right]$$

$$|V_i| < V_e \rightarrow \psi_2 = 0$$

$$\Gamma_2 = -\frac{\alpha_0^2}{\omega\tau_0^2}\left(\frac{\sigma_0}{\sigma_1}\right)^2\left[\frac{\rho_0}{\sigma_0}\frac{\partial\sigma}{\partial\rho}r_2 + \frac{h_0}{\sigma_0}\frac{\partial\sigma}{\partial h}\theta_2 - 2\frac{\sigma_1}{\sigma_0}\right]r_1v_1$$

Because of the normalization, the boundary conditions for the steady flow are simply

$$v_1 = r_1 = \theta_1 = 1 \text{ at } \xi = 0 \tag{16}$$

For steady flows that are everywhere supersonic, no hydrodynamic disturbance can propagate to the channel entrance from downstream regions. Then for such flows the boundary conditions for the stability analysis are

$$v_2 = r_2 = \theta_2 = 0 \text{ at } \xi = 0 \tag{17}$$

where such essentially spurious effects as unsteadiness in the gas supply have been neglected. These conditions do not mean that there is no disturbance at the inlet, but only that that part of the disturbance that propagates through the load circuit (i.e., electric current and field) can be there. The boundary conditions for subsonic flow are more subtle and not discussed here.

The generator terminal (Hall) voltage, and hence the external impedance $Z$, is determined by integrating the axial electrical field over the length of the machine; i.e., for $0 \leq \xi \leq 1$. This field may be expressed in terms of the solution of Eqs. (10–15) by means of Ohm's law. Separating as before the steady and perturbation contributions, one obtains

$$V_i > V_e \rightarrow \frac{dZ_1}{d\xi} = \frac{\omega\tau_0^2L}{\alpha_0\sigma_0A_0}\left[-\alpha_0\frac{\sigma_0}{\sigma_1}\frac{1+\omega\tau_1^2}{\omega\tau_0^2}r_1v_1 + \frac{\omega\tau_1}{\omega\tau_0}\left(v_1 - \frac{V_e}{u_0Bd}\right)\right]$$

$$|V_i| < V_e \rightarrow \frac{dZ_1}{d\xi} = \frac{\omega\tau_0^2L}{\alpha_0\sigma_0A_0}\left[-\frac{\alpha_0}{\omega\tau_0^2}\frac{\sigma_0}{\sigma_1}r_1v_1\right] \tag{18}$$

$$V_i > V_e \rightarrow \frac{dZ_2}{d\xi} = \frac{\omega\tau_0^2L}{\alpha_0\sigma_0A_0}\left\{\frac{\omega\tau_1}{\omega\tau_0}v_2 + \left[\frac{\rho_0}{\omega\tau_0}\frac{\partial\omega\tau}{\partial\rho}\times\left(v_1 - \frac{V_e}{u_0Bd} - 2\alpha_0\frac{\sigma_0}{\sigma_1}\frac{\omega\tau_1}{\omega\tau_0}r_1v_1\right) + \alpha_0\left(\frac{\sigma_0}{\sigma_1}\right)^2\times\frac{1+\omega\tau_1^2}{\omega\tau_0^2}r_1v_1\frac{\rho_0}{\sigma_0}\frac{\partial\sigma}{\partial\rho}\right]r_2 + \left[\frac{h_0}{\omega\tau_0}\frac{\partial\omega\tau}{\partial h}\left(v_1 - \frac{V_e}{u_0Bd} - 2\alpha_0\frac{\sigma_0}{\sigma_1}\frac{\omega\tau_1}{\omega\tau_0}r_1v_1\right) + \alpha_0\left(\frac{\sigma_0}{\sigma_1}\right)^2\frac{1+\omega\tau_1^2}{\omega\tau_0^2}r_1v_1\frac{h_0}{\sigma_0}\frac{\partial\sigma}{\partial h}\right]\theta_2 - \alpha_0\frac{\sigma_0}{\sigma_1}\frac{1+\omega\tau_1^2}{\omega\tau_0^2}r_1v_1\right\}$$

$$|V_i| < V_e \rightarrow \frac{dZ_2}{d\xi} = \frac{\omega\tau_0^2L}{\alpha_0\sigma_0A_0}\left\{\alpha_0\frac{\sigma_0}{\sigma_1}\frac{r_1v_1}{\omega\tau_0^2}\times\left[\frac{\sigma_0}{\sigma_1}\frac{\rho_0}{\sigma_0}\frac{\partial\sigma}{\partial\rho}r_2 + \frac{\sigma_0}{\sigma_1}\frac{h_0}{\sigma_0}\frac{\partial\sigma}{\partial h}\theta_2 - 1\right]\right\} \tag{19}$$

where $Z_1$ is the ratio of the steady voltage to the steady current $J_0$, and $Z_2$ is the ratio of the perturbation voltage to the perturbation current. Should $V_i < -V_e$ at some station in the machine, the transverse current changes sign and that section of the machine becomes an accelerator rather than a generator. The formal expressions for the $\psi$'s, $\Gamma$'s, and $Z$'s are the same as for the case $V_i > V_e$ except that $V_e$ is replaced with its negative.

The eight ordinary differential Eqs. (10–17) are a complete description of both the steady behavior of the channel and its stability against axial magneto-acoustic waves. It may be noted that these equations separate in groups so that it is possible to determine the steady behavior from the solution of Eqs. (10–12) first and then use these results for the coefficients in the dynamical perturbation Eqs. (13–15), and finally evaluate the integrals implied in Eq. (17) to answer the stability question. However, Eqs. (13–15) require numerical treatment so that it is more convenient to solve all eight equations simultaneously.

Besides the parameters $S$ and $\alpha_0$, and the specification of the inlet gas state, the equations involve a number of coefficients which describe the plasma. These include the 5 independent first- and second-order derivatives of the pressure with respect to the state variables, and the conductivity and Hall parameter and their first derivatives. It is also necessary to specify the channel core area $a(\xi)$ and the electrode drop parameter $V_e/u_0Bd(\xi)$. A computer program has been developed that has among its inputs eleven two-dimensional tables for the plasma properties and a one-dimensional table

for $a(\xi)$; it was assumed $d \propto a^{1/2}$. This program may be used to predict the stability of specific Hall generators with respect to axial magneto-acoustic waves. Two examples of this use are discussed under the heading "Specific Machines Under Various Loads." Before those results are presented, the application of the method to a general class of somewhat idealized generators is considered.

## Idealized Stability Map

The very specificality of the treatment described here, although necessary to provide realistic stability estimates, causes the treatment to be a poor vehicle for revealing any general insights into the nature of the possible instability and the isolation of the most relevant factors leading to instability. Certain simplifying assumptions facilitate the generation of surveyable results.

For an ideal gas with constant heat capacities, the equation of state is

$$p = [(\gamma - 1)/\gamma]\rho h \tag{20a}$$

where $\gamma$ is the ratio of heat capacities. For this gas, the five two-dimensional tables of pressure derivatives may be replaced with simple analytical expressions involving the single parameter $\gamma$. The electrical transport properties of a number of gases may be approximated by the expressions

$$\sigma = \sigma_0(h/h_0)^N \tag{20b}$$

$$\omega\tau = \omega\tau_0(\rho_0/\rho) \tag{20c}$$

Making these assumptions leads to the replacement of six two-dimensional tables with analytic expressions involving only the parameter $N$. The only inlet conditions that need be specified are $u_0h_0^{-1/2}$, $\omega\tau_0$, $\alpha_0$, and $S$. In place of $u_0h_0^{-1/2}$, it is convenient to introduce the entrance Mach number $M_0 = u_0[(\gamma - 1)h_0]^{-1/2}$.

The stability calculation yet requires the specifications of the core area $a(\xi)$. Rather than choosing an arbitrary but fixed area contour that would result in different gradients of the steady flow variables for different values of $S$ (and the other input parameters), and no doubt lead to quite poor generator design for some $S$ values, the values of $a(\xi)$ were chosen such that the enthalpy of the steady flow was uniform, i.e.,

$$\theta_1 = 1 \tag{21}$$

for all cases considered. This is accomplished by setting $d\theta_1/d\xi = 0$ in Eqs. (11) and (12), solving them for $r_1$ and $v_1$, and computing $a(\xi)$ from Eq. (10). This particular choice was made, because [with Eq. (20)] it leads to a constant loading parameter and approximately constant electrical efficiency throughout the channel. Since the enthalpy of the gas does not change, any electrical energy delivered to the load must be extracted from the kinetic energy of the gas. Defining $\eta$ as the ratio of the power delivered to the load to total energy flux in the flow at the channel entrance yields for this case

$$\eta = (u_0^2 - u_f^2)/(2h_0 + u_0^2) \tag{22}$$

where $u_f$ is the gas speed at the channel exit.

The equations have been solved and the perturbation impedance $Z_2$ computed for a spectrum of input parameters. Typical results for the impedance are plotted in Fig. 1. The solid curve is the locus of the complex impedance consistent with a perturbation of (real) frequency $\omega$ as $\omega$ varies from 0 to 10 $u_0/L$. All impedances in the right half plane can be synthesized with passive elements, but active elements (energy sources) are required in the left half plane. Thus, this particular generator is absolutely stable against both extremely low- and high-frequency perturbations of this type, since to simply maintain such a perturbation without

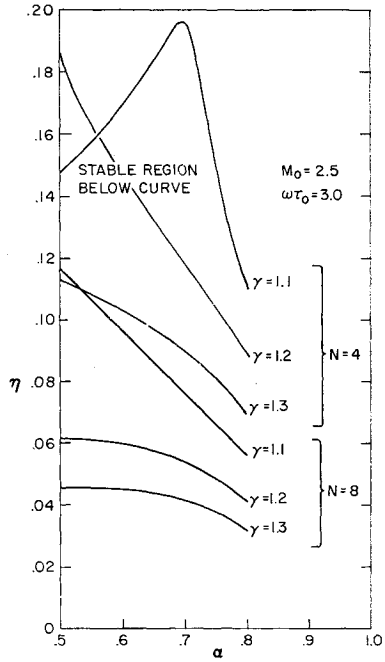


**Fig. 2 Absolute stability map for idealized generator: fraction of energy flux converted vs load parameter.**

growth requires an active element in the external circuit. However, for angular frequencies $\omega$ such that $1.4(u_0/L) < \omega < 2.1(u_0/L)$ this generator may be either stable or unstable, depending on the nature of the external circuit. If the load impedance at the frequency in question lies inside the spiral locus the system will be unstable, whereas it will be stable for load impedances outside. This interpretation may be confirmed and an estimate of the growth rate of the instability obtained by redoing the calculation for perturbations that grow or decay; i.e., for complex values of $\omega$. The dashed curves of Fig. 1 are the result of such a calculation. The curve inside the solid spiral has a negative imaginary part and hence corresponds to a growing disturbance, whereas that outside represents a decaying one. Thus, if the external impedance coincides with a point on the inner curve at a particular frequency, a disturbance of this frequency will grow with a characteristic growth time of 20 flow times. Although this growth is slow compared to the flow time or disturbance frequency, it is of course extremely rapid on the time scale of most practical applications of magnetohydrodynamic generators.

The general scale of impedance curves such as Fig. 1 increases with the machine length as measured by $S$ or equivalently $\eta$. Sufficiently short machines are absolutely stable. If the machine discussed in Fig. 1 were shortened so that $\eta = 0.070$ the solid curve would be tangent to the imaginary axis; this would then be the highest value of $\eta$ (i.e., largest machine) for which a generator of this description is absolutely stable. Similar calculations for various values of $\alpha_0$, $\gamma$, and $N$ lead to the stability map presented in Fig. 2, where the maximum value of $\eta$ for which a constant enthalpy generator is absolutely stable is plotted as a function of the load parameter $\alpha$. The increased tendency toward instability as $\alpha$ increases is primarily a reflection of the lowering of the power density as $\alpha$ increases towards $\alpha = 0.9$ (at which value the power density vanishes for $\omega\tau = 3$), so that the generator must become physically longer to generate the same power. The maximum stable $\eta$ generally slightly more than doubles as $N$ is decreased from 8 to 4, suggesting that the fluctuations of conductivity with enthalpy are the dominant mechanism of instability in this region. The specific heat ratio $\gamma$ (or better $\gamma - 1$) also seems to have an important influence on stability, though not as strong as $N$. A few calculations at other values of the inlet Mach number and Hall parameter not plotted here suggest that stability is less sensitive to

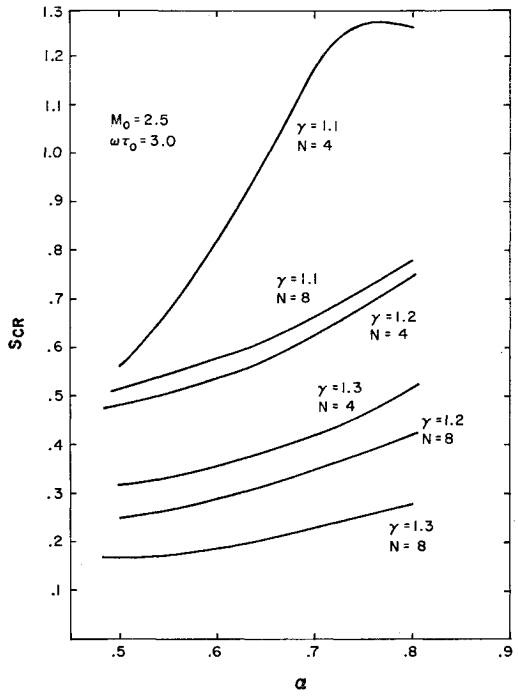


**Fig. 3 Absolute stability map for idealized generator: critical interaction parameter vs load parameter.**

these inlet conditions than it is to the plasma properties $\gamma$ and $N$. It may be noted that, typically, instabilities may develop in generators that extract about 10% of the thermal flux.

The instability possible above the curve for $\gamma = 1.1$, $N = 4$, $\alpha < 0.7$ is somewhat different than that possible above the other curves in that it is an instability at very low frequencies (especially 0) rather than over a limited resonant band bounded away from zero. This result may be interpreted as a positive slope to the generator voltage-current curve, or a negative internal resistance of the zero frequency Thevenin equivalent circuit. Actual instability still depends on the relation between this resistance and the internal load, but at zero frequency the external load is specified by the operating condition, and is proportional to $Z_1$ [Eq. (18)]. Thus, actual instability results if $Z_1 - Z_2(\omega = 0) < 0$.

If instead of the maximum value of $\eta$ for which these machines are absolutely stable, the largest value of the interaction parameter for absolute stability, $S_{cr}$ is plotted, the somewhat more orderly Fig. 3 is obtained. An examination of this figure reveals that $S_{cr}$ is closely proportional to $(\gamma - 1)^{-1}$, and indeed, except for the degenerate case of $\gamma = 1.1$ and $N = 4$ discussed above, all of the data represented on this figure can be represented by the correlation formula

$$S_{cr} \approx 0.8\alpha/N(\gamma - 1) \qquad (23)$$

within about 10%. It must be emphasized that this is purely an empirical relation based on Fig. 3, and no claim is made for its validity outside of the range of parameters considered in that data. In particular, the dependence on $\alpha$ is rather suspect, since even over the very limited variation of $\alpha$ considered in Fig. 3, the curvature of $S_{cr}$ vs $\alpha$ is evident. It is expected that the coefficient 0.8 varies significantly with $M_0$. Much variation with $\omega\tau_0$ is not expected however, since an examination of Eqs. (10–17) reveals that $\omega\tau_0$ enters only in the combination $(1 + \omega\tau_1^2)/\omega\tau_0^2$, and since $\omega\tau_1 > \omega\tau_0$, this combination cannot vary much even for $\omega\tau_0$ only modestly greater than unity.

The very features that permit the present analysis to be used to evaluate over-all machine stability make it quite difficult to seek out a justification for the success of correlation (23), these features being the treatment of a proper boundary-value problem and the integration over the entire machine, taking into account the varying gradients and parameters. A detailed comparison of the cases $\gamma = 1.1$, $N = 8$ with $\gamma = 1.2$, $N = 4$ at $\alpha = 0.6$ is suggestive, however. Under conditions (21), Eqs. (10–12) are independent of $N$ and only weakly dependent on $\gamma$ (i.e., $\gamma$ rather $\gamma - 1$ is involved, so that the 2 cases compared here differ by 10%), so that the equilibrium conditions and gradients on a distance scale normalized by $S$ are essentially the same for these two cases. Under these conditions, the perturbation growth as measured by any of the quantities $|v_2|$, $|r_2|$, or $|\theta_2|\ (\gamma - 1)^{-1}$ on this same scale are essentially the same for the two cases. It must be noted here that this remark does not justify the adiabatic approximation of primitive wave-growth theories which assume $v_2 \simeq r_2 M^{-1}$, $\theta_2 \simeq (\gamma - 1)r_2$ appropriate for an up-stream acoustic wave in the absence of magnetohydrodynamic interaction and gradient effects. Indeed, for this particular case, $|\theta_2| \sim 7(\gamma - 1)\ |r_2|$ and $|v_2| \sim 4M_0^{-1}|r_2|$. Further, even the relative importance of the various terms contributing to perturbation growth varies substantially with position ($\xi$), with the gradient terms dominating at the exit. Thus, all that can be said presently toward understanding correlation (23) is that conductivity fluctuations are the principal mechanism of perturbation growth in the range of parameters considered, and that the enthalpy fluctuations appear to be proportional to $\gamma - 1$, so that $S_{cr} \propto N^{-1}(\gamma - 1)^{-1}$. It is not to be expected that this simple correlation could embrace situations with very different equilibrium flows, or cases where the principal mechanism of perturbation growth was not conductivity fluctuations (if any such can lead to instability). The specific calculations reported in the next section also shed some oblique light on this point.

A comparison of the order of magnitude of the critical interaction parameter computed by the present theory with earlier wave growth calculations is instructive. The most direct comparison is with the work of Locke and McCune,[3] who plot the wave growth rate normalized by the interaction parameter for the fastest growing wave mode (the slow downstream wave) as a function of $\gamma$ for $N = 10$, $\alpha = 0.75$, and $M_0 = 3$, values that are close to those for which correlation (23) was observed to hold. Assuming that this correlation is approximately correct for these slightly different values yields values of the exponential growth rate $k_i L$, varying from 0.6 to 1.8 at the critical interaction parameter as $\gamma - 1$ varies from 0.1 to 0.6. Although the limitations of the wave growth theory, especially the fact that it is limited to short wavelengths whereas the wavelength of the disturbance that contributes most critically to the instability characterized by correlation (23) is of the order of the machine length, invalidate any more detailed conclusions, it seems reasonable to conclude that wave growth rates of the order of unity are enough to lead to machine instability. The physical interpretation is that the load feed-back path permits continual growth that is not terminated when an individual wave packet is convected from the channel.

## Specific Machines under Various Loads

Although stability maps of the type discussed previously do give at least an approximate indication of the possibility of instability for generators that approach the model implied by Eqs. (20) and (21), other types of machines may present rather different characteristics, and resort must be made to the general apparatus of Eqs. (10–17). To illustrate, calculations specific to the mathematic models of two particular machines are presented. The first is the Avco Everett Mark II combustion driven experimental facility whose operation and model is reported in Ref. 6. Electrical power output of about 1 Mw at a thermal heat flux of about 30 Mw have been achieved. A one-dimensional flow model with suitable allowance for

electrode voltage drop and a self-consistent boundary-layer calculation has been shown to be in good agreement with the experiments at typical operating conditions. The core area calculated by this model, along with the results of thermodynamic equilibrium calculations for the appropriate combustion products, have been used as inputs to the present stability calculations; perturbation impedance plots are presented in Fig. 4. The results for three different values of steady current $J_0$ are presented and distinguished in the figure by the load resistance that corresponds to each current; they range from the lightly loaded 3.6Ω case to a 13Ω case, which corresponds about to maximum power operation. A wide margin of absolute stability is indicated for each case, i.e., all points lie far into the active load zone.

It is instructive to attempt to locate these results on Figs. 2 and 3. Such an attempt is reasonable since this machine was indeed designed to have only small gradients in enthalpy and loading parameter; for the 9Ω load the model predicts a 5% rise in enthalpy and an 18% decrease in load parameter over the length of the channel. The equilibrium calculation for the appropriate combustion products indicates that Eqs. (20b, c) are indeed a good approximation for this case with $N = 4$. The derivatives of pressure with the state variables are not completely consistent with those implied by Eq. (20a) for any value of $\gamma$, as they imply a weaker but higher-order dependence of $p$ on $h$. However, if the gas is modeled by an ideal gas with temperature-dependent heat capacities, the calculated derivatives imply a (local) heat capacity ratio $\gamma \cong 1.12$. The initial loading parameter for the 9Ω case is $\alpha_0 = 0.743$, falling to $\alpha = 0.62$ at the exit. If $\eta$ is evaluated as the ratio of the total change in energy flux in the core to the input flux a value $\eta = 0.05$ is obtained. (Not all of the energy extracted from the core is available as electrical output, but some is lost through the electrode drop mechanism.) Locating this operating point on Fig. 2 suggests that this machine has a wide margin of stability, in agreement with the specific calculation represented by Fig. 4.

The interaction parameter of this model generator is $S = 0.88$. Simply locating this point on Fig. 3 would leave considerable doubt as to the stability of the generator, considering the uncertainties in $\gamma$ and the effective value of $\alpha$. It is strongly suggested that were the gas somewhat different, having a higher value of $N$ or $\gamma$, the possibility of instability would be easily reached, as opposed to the suggestion of Fig. 2. However, there is no direct contradiction, either for the specific case under consideration, which is uncontroversially stable by Fig. 4, or for somewhat modified machines, since the relation between $\eta$ and $S$ depends on $\gamma$, $\alpha_0$, $N$, as well as channel contour and electrode drop, among other parameters. Perhaps the wisest conclusion that can be drawn from this near contradiction is that Figs. 2 and 3 must be used with caution, even for machine designs that diverge from the idealizations [e.g., Eqs. (20) and (21), $V_e/u_0Bd \ll 1$] on which they were based by relatively small amounts.

The second example presented here is related to the Avco Everett high interaction inert gas generator and analytical model reported in Ref. 7. A de facto degradation of Hall parameter had to be introduced into the model to obtain approximate agreement with experiment; that degradation factor was not adopted in the present analysis of the model's

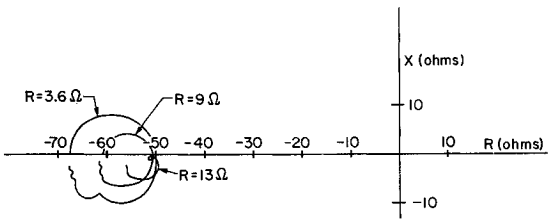


**Fig. 4 Complex perturbation impedance for the Mark II combustion-driven Hall generator at 3 loads.**

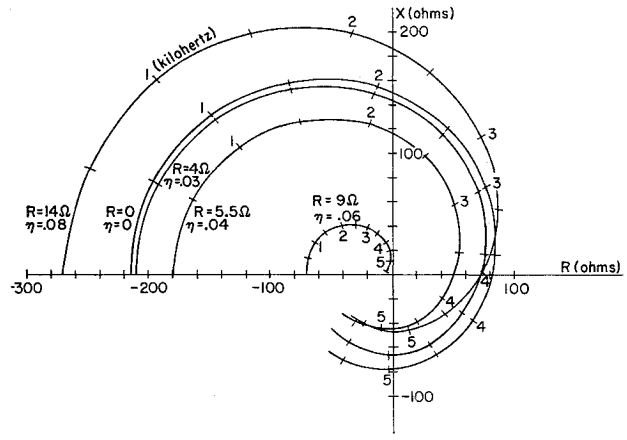


**Fig. 5 Complex perturbation impedance for the high-interaction Hall generator at 5 loads.**

stability. This model has a relatively high interaction parameter $S = 1.25$ and the design tended toward constant velocity rather than constant enthalpy. In the particular configuration analyzed electrode-drop phenomena are quite significant, with $V_e/u_0Bd \cong 0.7$. Under these conditions, the enthalpy can vary by 25% through the machine and the loading parameter varies widely. A number of different loading conditions were studied, ranging from over-all short-circuit to a case loaded so heavily that the machine would certainly stall. In the latter case, the loading parameter varied from $\alpha_0 = 0.12$ to $\alpha = 0.6$, and the transverse current decayed monotonically to zero. In the short-circuit case, the loading parameter varies from $\alpha_0 = 0.14$ to $\alpha = 1.7$, and three regions can be distinguished within the machine; an initial generator portion which powers an exit accelerator region, which is separated from the generator by an idling regioning which the electrode drop prevents sensible transverse currents of either sign. The perturbation impedance plot for five different loadings are presented in Fig. 5. The various curves are labeled not only with the load resistance, but also with the calculated ratio of the electrical output to the input thermal flux; because of the high electrode drop, values of $\eta$ calculated from the change of core energy flux would be substantially larger, ranging upward to 15% for the most heavily loaded case. Also indicated along the curves is the perturbation frequency in KHz.

The most striking aspect of Fig. 5 is that this model is subject to potential instability at both low and very high loading levels, but absolutely stable at a certain intermediate level. It would be very difficult to predict this behavior solely on the basis of Fig. 2 or 3: even a qualitative understanding requires cognizance of the three regions noted previously in the short-circuited case. For all of the cases presented here, the perturbation growth over the initial generator region is essentially the same. This region fills the heavily loaded machine. In this case, the perturbation grows essentially exponentially throughout the channel, attaining a substantial magnitude at the exit, resulting in possible instability under unfavorable frequency-phase circumstances. However, as the loading is decreased an idling region moves up the machine from the exit; in this region the perturbation does not grow but decays slowly instead. In the 9Ω case, this region occupies the final 20% of the channel and perturbations sufficiently large to lead to instability do not occur. At loads of 6Ω or less an accelerator region appears at the channel exit; in such regions the nature of the perturbation changes rapidly, with a strong tendency toward instability evident. In circumstances such as these, an over-all stability assessment clearly requires an integration over the full channel, such as provided by the present formalism.

Notice also that the load resistances are generally much smaller than the magnitude of the perturbation impedances plotted in Fig. 5. In particular, for the four cases indicating potential instability, the load resistances lie inside the perturbation impedance spiral. Thus, if the machine is terminated with a simple resistance, the generator should actually be unstable for the loads that are indicated as being potentially unstable in this illustration.

## Stabilization

A careful distinction has been made between absolute stability and stability that depends on the load circuit. The present results suggest that any generator can be made stable against magneto-acoustic waves by the insertion of an appropriate filter in the load circuit. A sufficient (it is more restrictive than necessary) design criteria for a stabilizing filter, in terms of perturbation impedance charts like Figs. 1, 4, and 5, is that the load impedance lies outside of the perturbation impedance locus for all frequencies for which the real part of the perturbation is positive, and that the load impedance corresponds to the loading condition at zero frequency. One such filter is a sufficiently large pure inductor in series connection with the loading resistor. For example, the machine discussed by Fig. 5 can be stabilized at all loads less than 14Ω (the entire useful range) by connecting a 15 mh inductance in series with the load. Then, for frequencies above 2000 Hz, the load reactance will be greater than 190Ω and hence outside the region of perturbation growth. More sophisticated filter design permits stabilization with elements of lower $Q$.

One apparent exception to the theorem that all machines can be stabilized is any generator that exhibits instability at zero frequency with $Z_1 - Z_2(w = 0) < 0$. However, since any generator must be characterized by a positive short-circuit current and open-circuit voltage, for any given load resistance, there must be at least one operating point where the generator voltage-current characteristic is negative, so that $Z_1 - Z_2(w = 0) > 0$, and the machine is stable. In a sense then, the zero frequency instability is an artifact of the calculation scheme that has $\alpha_0$ as an input parameter, rather than the physical parameter load resistance.

One circumstance might exist in which stabilization attempts by load impedance control would be ineffective. It is possible that a disturbance injected at the channel entrance could grow so rapidly that it could become large enough to effect generator performance seriously before it was swept from the machine or controlled by a suitably filtered feedback signal through the load. The present analysis which assumes linear, basically continuous wave phenomena, is not appropriate for the discussion of such single pass disturbances.

As a filter in the load circuit may be used to stabilize an otherwise unstable generator, so too may a filter be used to promote the growth of a disturbance of a particular frequency in any generator that is not absolutely stable at that frequency. The present linear theory describes the initial growth rate of all disturbances, but unfortunately cannot describe the ultimate flow in an unstable generator, nor even suggest the nature of the nonlinearity that limits disturbance growth. Thus, it provides no predictions as to whether these instabilities can become a useful source of a.c. power. For the same reason, the diagnosis of an experiment possibly subject to these instabilities is less than certain.

## Comparison with Experiment

No experiments have been designed explicitly to confirm this theory. However several observations made of the operation of the Mark II[6] and high-interaction[7] generators may be cited, though the caution of the preceding paragraph must be observed. Large-scale ($\epsilon \sim 0.3$) voltage fluctuations with a characteristic frequency of a few KHz have been observed in the output of the high-interaction generator when it was terminated with a pure resistance. Such fluctuations are in accord with the present theory. During a single, minimally instrumented, experiment, an inductor, theoretically adequate to stabilize the generator, was connected in series with the load. The observed output voltage fluctuations increased by about a factor of two, but the order of magnitude increase in impedance at these frequencies implies that the fluctuation power decreased by a greater factor. Fluctuations are also observed in the output of the theoretically stable Mark II generator with resistive load. These fluctuations also have a period comparable to the gas flow time in this longer channel, and they are of a somewhat smaller relative amplitude than those observed in the resistively loaded high-interaction generator.

One possible explanation of these observations is that there is a source of fluctuations in these machines besides the instability considered here. One might imagine unsteadiness in the energy source or in the seeding process (though limited attempts to isolate such effects in the Mark II were unsuccessful). Such a source might be responsible for the observed Mark II fluctuations and for the fluctuations observed in the high-interaction machine with inductive load. The reduction in fluctuation level in the latter machine by the addition of the inductor could then be attributed to the complete elimination of the type of disturbance discussed in this paper.

Another speculation may be offered concerning the size of the observed fluctuations. In the resistively terminated high-interaction generator these corresponded to a 30% current fluctuation. If this current fluctuation is attributed to a disturbance of the type considered in this paper, relative conductivity fluctuations of 30% and Hall parameter fluctuations of 10% should occur near the middle of the channel, the fluctuation being much smaller near the channel entrance but larger at the exit. Rosa has considered the effect of nonuniformities in MHD generators and has concluded that nonuniformities of the geometry considered here (a nonuniformity in the stream direction in a Hall generator) causes a reduction in the effective Hall parameter without influencing the effective conductivity.[8] Although the details of Rosa's calculations are not applicable to a channel with large steady gradients, an order-of-magnitude estimate based on his results suggests that the 30% conductivity fluctuations deduced above could cause a reduction of Hall parameter of the order that was found necessary to describe the high-interaction generators steady performance. Because of the lower fluctuation level in the Mark II and especially because of the lower theoretical Hall parameter, no degradation in this parameter would be expected in this machine, and none has been observed.

## Conclusions

It has been demonstrated that Hall MHD generators may be unstable to magneto-acoustic waves. The dominant disturbances contributing to the instability have a period comparable to the gas flow time in the channel. It is suggested that instabilities may occur when the fastest growing pure waves exhibit a growth rate of order unity. This instability is more likely to occur in generators of high interaction or high fractional energy extraction than low, and also increases in probability with the sensitivity of the conductivity of the plasma to enthalpy changes and with the plasma's $\gamma$. Although no parameter, or set of parameters, that describe the dependance have been isolated, the equilibrium channel gradient distribution has an important effect on stability. An extreme example of this last effect was noted in the high-interaction generator, where the existance of even a very

short section of channel with accelerator-like action was decisive.

Finally, it may be pointed out that within the limitations of the linearization and geometrical assumptions, the formalism developed here is a general description of the time dependent Hall generator flow, and hence, has potential applications beyond the assessment of stability. In particular, the impedance function $Z_2(w)$ is the ratio of the change in terminal voltage to the corresponding change in output current, whatever the cause of these changes. Thus, this function completely describes the electrical behavior of the generator viewed as a linear, two-terminal black box; i.e., it is sufficient to characterize the generator as a circuit element within a larger network. One important application of this description is the analysis of a generator-inverter circuit to deliver a.c. power.

## References

[1] Velikhov, E. P., "Hall Instability of Current-Carrying Slightly-Ionized Plasmas," *Proceedings of the Symposium on Magnetoplasmadynamic Electrical Power Generation*, Newcastle upon Tyne, Great Britain, 1962, pp. 135–136.

[2] McCune, J. E., "Wave Growth and Instability in Partially Ionized Gases," *Proceedings of the International Symposium on Magnetohydrodynamic Electrical Power Generation*, Paris, 1964, pp. 523–538.

[3] Locke, E. V. and McCune, J. E., "Growth Rates for Axial Magneto-Acoustic Waves in a Hall Generator," *AIAA Journal*, Vol. 4, No. 10, Oct. 1966, pp. 1748–1751.

[4] Powers, W. L. and Dicks, J. B., "Transient Wave Growth in Magnetogasdynamic Generator," *AIAA Journal*, Vol. 6, No. 6, June 1968, pp. 1007–1012.

[5] McCune, J. E., "Linear Theory of an MHD Oscillator," *Advanced Energy Conversion*, Vol. 5, 1965, pp. 221–240.

[6] Teno, J., Brogan, T. R., and DiNanno, L. R., "Hall Configuration MHD Generator Studies," *Electricity from MHD*, Vol. 3, International Atomic Energy Agency, Vienna, 1966, pp. 603–614.

[7] Klepeis, J. E. and Olin, J. G., "Experimental Studies with an Arc-Driven Hall MHD Generator with Strong MHD Interaction," *Proceedings of Ninth Symposium on Engineering Aspects of Magnetohydrodynamics*, University of Tennessee, Space Institute, Tullahoma, Tenn., 1968, pp. 99–100.

[8] Rosa, R. J., "The Hall and Ion Slip Effects in a Non-uniform Gas," *The Physics of Fluids*, Vol. 5, 1962, pp. 1081–1090.